Australian Journal of Biomedical Research
(eISSN 3083-4708)

Original Article

Green synthesis of *Euphorbia hirta* Extract–Based Mesoporous Bioactive Glass Nanoparticles: Structural and Biological Insights toward Diabetes Treatment

Arul Sowmiya[1], Suresh Sasikala[1], Nagarajan Usharani[1]

[1]*Department of Molecular Analytics, Saveetha School of Engineering, Saveetha Institute of Medical and Technical Sciences (SIMATS), Chennai, Tamil Nadu, India*

Received: Dec 07, 2025
Accepted: Feb 21, 2026

Corresponding author's email: usharn2019@gmail.com

Abstract:

Euphorbia hirta is a novel medicinal plant with clinical applications that demonstrate antimicrobial, anti-inflammatory, and anticancer activity. Precisely, the state of the art of this plant has been extensively explored within the context of nanotechnology and its advancements. The all-inclusive efficiency of this plant can be achieved by incorporating metal nanoparticles. In this current study, plant extract-incorporated Mesoporous Bioactive Glass Nanoparticles (MBGNs) were prepared and characterized for controlled delivery toward diabetes Treatment. Moreover, a novel and holistic approach based on the synthesis, functionalization, and biological characterization of *Euphorbia hirta*-loaded MBGNs to evaluate their structural integrity and antibacterial efficacy was employed. MBGNs were synthesized via a sol–gel method, functionalized using APTES, and subsequently loaded with *Euphorbia hirta* extract. Structural characterization using SEM, EDX, FTIR, and XRD was performed, and a significant zone of inhibition was achieved to execute antibacterial activity. MBGNs exhibited notable antibacterial activity, particularly against *S. aureus* and *A. baumannii*. However, functionalization and extract loading led to poor antibacterial activity, likely due to hindered ion release and altered surface interactions. While *Euphorbia hirta*-loaded MBGNs demonstrate structural and chemical stability, surface modifications may compromise antibacterial activity. These findings emphasise the importance of striking a balance between structural alteration and functional performance. These results provide valuable insights for designing and scoping the development of multifunctional nanocarriers in biomedical applications, particularly for diabetes wound healing and localized antimicrobial therapies.

Keywords: *Euphorbia hirta*; MBGN; Antibacterial Activity; Phytochemical Delivery; Sol–Gel Synthesis

Introduction

MBGNs are bioceramics typically synthesised within the glass network system made of calcium silicate, owing to their large surface areas. MBGNs feature a highly ordered network of channel-like mesopores, typically 5-20 nm in diameter, along with substantial pore volume. Unique mesostructured nanoparticles have proven to be a promising platform for drug and biomolecule delivery[1, 2]. Specifically, subsequent hydrolysis and condensation resulted in the formation %of MBGs, a significant precursor of silicate. Importantly, the ion-release profile of MBGs can play a critical role in the micro-environment of diabetic ulcers, where impaired healing is often a challenge. The controlled release of therapeutic ions can enhance bioactivity and potentially improve wound-healing outcomes in patients with diabetes [3].

MBGNs exhibit rapid bioactivity. This is mainly due to the release of large amounts of silicon (Si^{4+}) ions. The release of calcium (Ca^{2+}) ions also supports cell proliferation and enhances osteogenic activity. These properties make MBGNs highly effective in bone regeneration and related applications. For example, MBGNs with dimethyl oxalyl glycine show angiogenic activity in stem cells. Doxorubicin-loaded MBGNs serve as a potential anticancer agent [4, 5].

Nanosized pharmaceuticals have shown strong antibacterial and antifungal properties. This makes them suitable for inclusion in medical devices such as bone cements, surgical instruments, and wound dressings. Silver nanoparticles (AgNPs) have recently shown antiviral activity against infectious viral particles. However, the clinical use of these nanoparticles raises concerns. Specifically, AgNPs exhibit high cytotoxicity toward mammalian cells, limiting their safe use in medicine. As a result, while antibacterial applications have developed rapidly, antiviral nanoparticle therapies are limited by safety issues [6-10].

As a potential alternative, *Euphorbia hirta* offers significant antimalarial, antifungal, antifertility, antispasmodic, sedative, anti-asthmatic, anthelmintic, and antibacterial properties [11]. Hence, in this study, we have functionalized the ethanolic extract of *Euphorbia hirta* with amino-group-functionalized MBGNs (58% SiO2, 37% CaO, 5% P2O5) to evaluate its antibacterial activity. We hypothesized that the amino-functionalization would improve the efficacy of the extract by enhancing its stability and bioavailability, thereby facilitating a more efficient delivery of its antibacterial properties. This hypothesis guided our approach to the preparation and characterization of the functionalized MBGNs.

Materials and Methods

Formation of MBGNs nanoparticles

Mesoporous Bioactive Glass Nanoparticles (58S) were made from an optimised composition of SiO2:CaO:P2O5 (58:37:5 (weight ratio)). The synthesis used a sol-gel-modified co-precipitation technique. Ethanol was mixed with 21 mM Tetraethyl orthosilicate (TEOS) at pH 2 and stirred at 400 rpm for 20 min. Calcium hydroxide solution (13 mM) was then added to the TEOS solution. The mixture was combined with ammonium dibasic phosphate (1.72 mM) while maintaining a pH of 11, as monitored with a calibrated pH meter. After stirring for 48 hours, the precipitates were collected and filtered. The samples are washed and stored at 60 °C. Further calcination at 680°C produced dried MBGNs [12].

Collection of plant material

Leaves from *Euphorbia hirta* were collected and thoroughly washed with deionised water. They were dried at 37°C, then pulverised using a mechanical grinder. The fine powder was separated and stored at room temperature [13].

Plant extraction method

The plant extract solution was prepared by mixing 20 g of fine powder with absolute ethanol and incubating overnight at -4°C. The solution was subsequently agitated and filtered through Whatman filter paper and stored [14].

Surface functionalization of MBGNs with Euphorbia hirta extract

The MBGN surface's amino group was functionalized with (3-aminopropyl) triethoxysilane (APTES). Pure MBGNs were segregated by centrifugation at 13,000 rpm for 30 min in a 95% acetone solution. Following activation with acetone, 25 mg of MBGNs were dispersed in 25 mL of 95% ethanol. The functionalized nanoparticles were isolated through centrifugation and then dried for further analysis [15].

The slow stirring of *Euphorbia hirta* with MBGNs yielded a composite of plant-incorporated MBGNs. Specifically, 5 mg of dried extract was dissolved in 5 ml of ethanol (10% V/V) for 24 h. Next, the solution was subjected to ultrasonic treatment for 5 min with 50 mg of Mesoporous bioactive glass nanoparticles. Subsequently, the solution was stirred at 400 rpm for a specific duration. Finally, the product was centrifuged at 2000 rpm and dried under ambient conditions. The maximum loading efficiency of Euphorbia hirta constituents onto the MBGNs was

anticipated, providing a crucial metric for correlating with the biological activity observed later in the study [16].

Characterization

Scanning Electron Microscope

The morphological variation and formation of mesoporous bioactive glass nanoparticles (MBGNs) were confirmed using Field Emission Scanning Electron Microscopy (FE-SEM) after synthesis and functionalization with Euphorbia hirta extract, and the results were compared with those of the unmodified control sample.

Structural and chemical analysis

The elemental composition of mesoporous bioactive glass nanoparticles (MBGNs) was analysed by energy-dispersive X-ray spectroscopy (EDX). Furthermore, the functional group interactions and complex formation between MBGNs and Euphorbia hirta extract were confirmed by Fourier Transform Infrared Spectroscopy (FTIR). The FTIR spectra were recorded in absorbance mode over the range 4000–650 cm^{-1}. In addition, X-ray diffraction (XRD) was performed to investigate the structural characteristics and phase composition of MBGNs.

Antibacterial activity

The antibacterial activity of MBGN, functionalized MBGN, and *Euphorbia hirta*-loaded MBGN was evaluated using the agar well diffusion method against *Staphylococcus aureus, Acinetobacter baumannii, Escherichia coli, Klebsiella pneumoniae,* and *Pseudomonas aeruginosa*. Control samples containing silver nanoparticles (0.5-10 mg/mL) were incubated overnight. The zone of inhibition (in mm) produced against the test microorganisms was recorded and compared with the control zone.

Statistical Analysis

The experiments were performed in triplicate; all results are represented as mean, standard deviation, and standard error.

Results

Morphological analysis - Scanning Electron Microscope

The SEM images in Figure 1 (a-c), Figure 2 (a-c), and Figure 3 (a-c) depict MBGNs, Functionalized MBGNs, and Euphorbia hirta-loaded MBGNs at varying magnifications. It is clear from these micrographs that the MBGNs exhibit spherical particles with rough, mesoporous structures, as noted [17, 18]. The formation of these spherical particles is significantly affected as a function of the difference in the reaction mixture and pH conditions [12]. Upon loading the MBGNs with Euphorbia hirta extract, a notable change in morphology occurs. At a 300 nm scale, the Euphorbia hirta-loaded MBGNs exhibit increased roughness compared to unloaded MBGNs and functionalized MBGNs. This uneven, denser morphology likely results from the presence of bioactive material, as observed in the *Euphorbia hirta*-loaded samples. The altered surface characteristics suggest the formation of surface layers upon loading functionalized MBGNs, resulting from the interaction between the plant extract and the nanoparticle surface. These changes in surface morphology could enhance or inhibit ion release and, in turn, affect cell adhesion properties, thereby influencing the biological functionality of MBGNs in therapeutic applications.

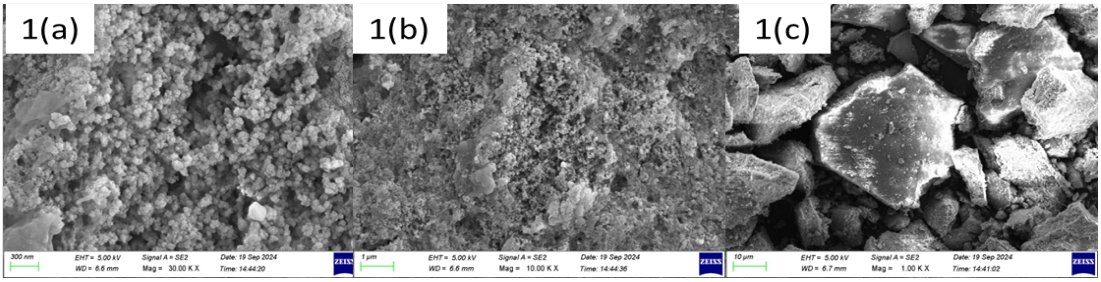

Figure 1. (a-c) SEM images of Mesoporous Bioactive Glass Nanoparticles.

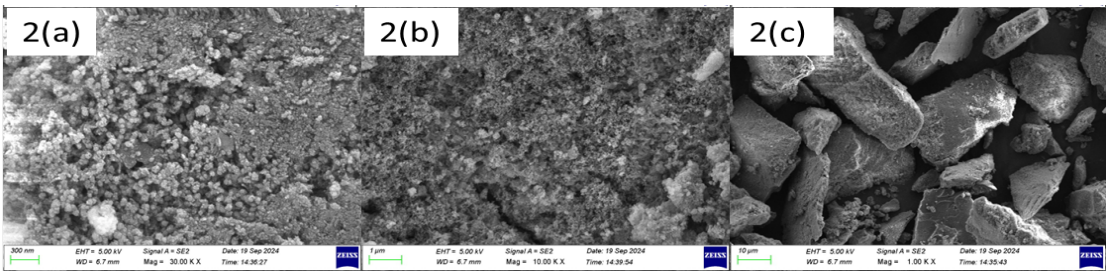

Figure 2. (a-c) SEM images of Functionalized Mesoporous Bioactive Glass Nanoparticles.

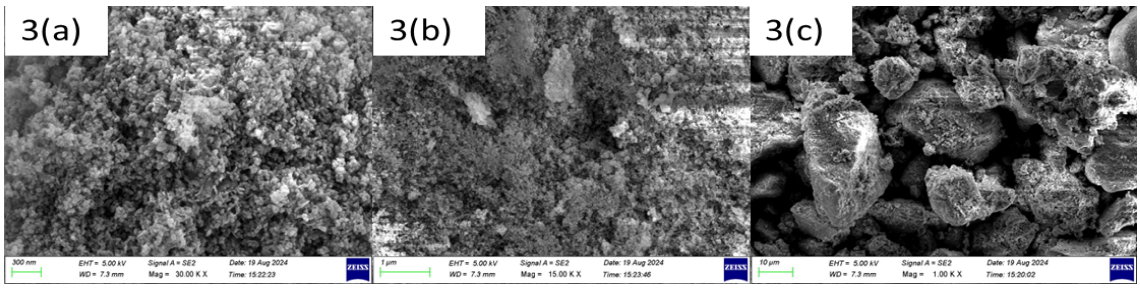

Figure 3. (a-c) SEM images of *Euphorbia hirta* loaded with Mesoporous Bioactive Glass Nanoparticles.

Chemical analysis

EDX

Figure 4 (a-c) displays the EDX spectra of synthesised MBGNs, functionalized MBGNs, and *Euphorbia hirta*-loaded mesoporous bioactive glass nanoparticles, confirming the traces of Si, Ca, and P in the prepared nanoparticle system. The chemical composition was calculated based on the obtained atomic ratios and is shown in the table in Figure 4(a-c). The amalgamation of Si, Ca, and P has a redefined crystallised elemental group when compared with the control MBGN.

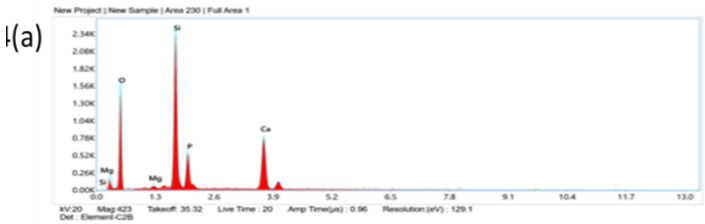

Element	Weight %
O K	53.30
Mg K	0.76
Si K	21.47
P K	7.85
Ca K	16.62

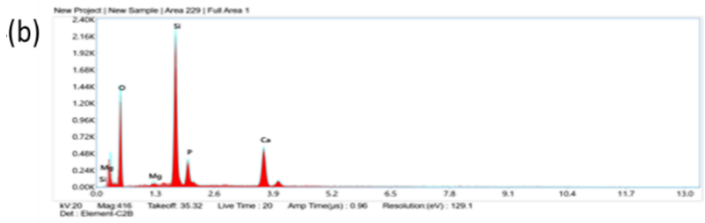

Element	Weight %
O K	53.98
Mg K	0.83
Si K	24.30
P K	6.62
Ca K	14.27

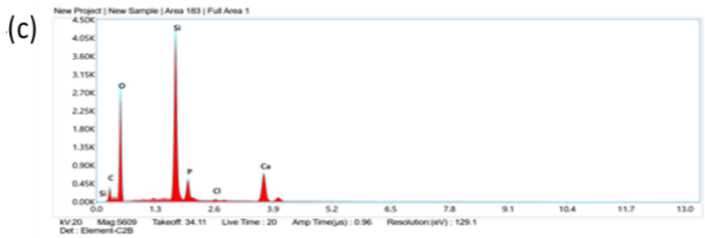

Element	Weight %
C K	12.16
O K	52.45
Si K	21.93
P K	4.48
Cl K	0.26
Ca K	8.73

Figure 4. EDX spectra of (a) MBGN, (B) Functionalized MBGN, (C) *Euphorbia hirta* – loaded MBGN.

Functional analysis

The functional annotation of MBGNs by APTES was confirmed using FTIR. In the literature, bands observed at 1067 cm-1 and 1030 cm-1 are attributed to MBGNs containing manganese and magnesium [19] [20]. These findings have a good correlation with the literature. An intense peak observed at 1028 cm-1, 1021 cm-1, and 1028 cm-1 for 58s MBGN, functionalized 58s MBGN, and *Euphorbia hirta*-loaded 58s MBGN, respectively, corresponds to Si-O-Si asymmetric stretching vibrations. Additionally, a shallow band at 693 cm-1 was observed in both functionalized 58s MBGN and *Euphorbia hirta*-loaded 58s MBGN, confirming the successful incorporation of functional groups via APTES. FTIR spectra of MBGN, functionalized MBGN, and *Euphorbia hirta*-loaded MBGN are shown in Figure 5.

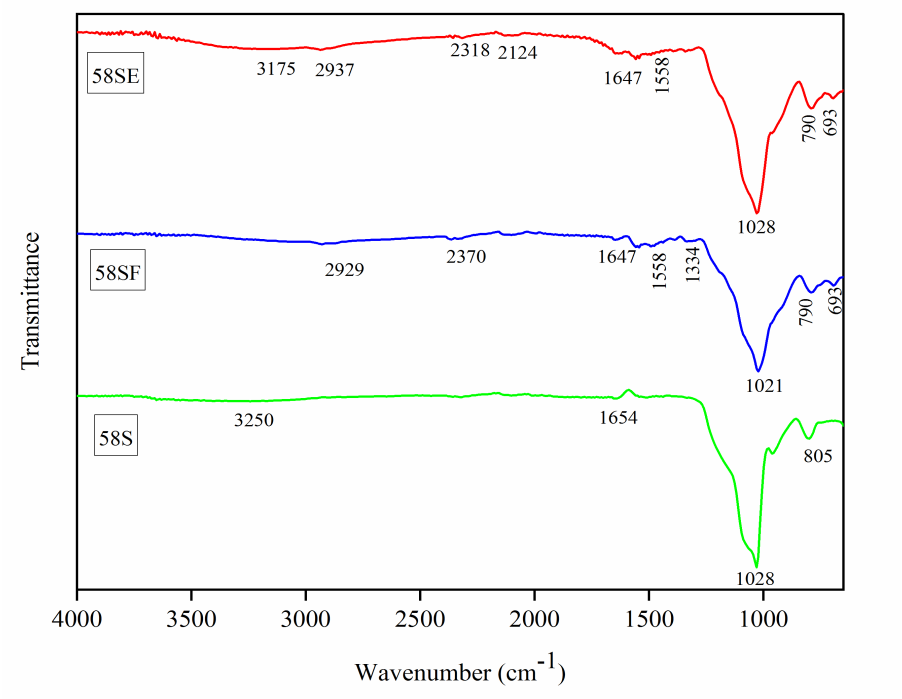

Figure 5. FTIR spectra of MBGN, Functionalized MBGN, and *Euphorbia hirta*-loaded MBGN.

XRD Analysis

Figure 6 illustrates the XRD patterns of MBGNs functionalized with *Euphorbia hirta* extract. The absence of sharp diffraction peaks in all samples confirms their amorphous nature. A broad diffraction halo observed between 30° and 35° (2θ) is characteristic of the disordered atomic arrangement typical of glassy materials. The shallow diffraction peak confirmed the amorphous nature of functionalized MBGNs and Euphorbia hirta-loaded MBGNs with no crystalline peaks. indicating that neither surface functionalization nor extract loading altered the inherent amorphous structure of the MBGNs.

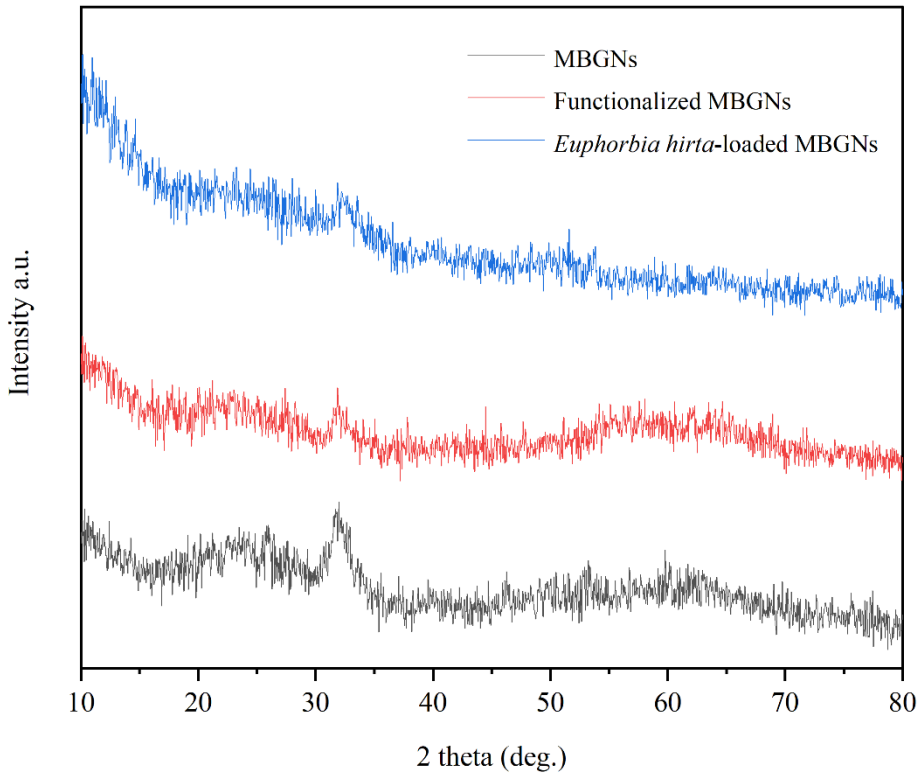

Figure 6. XRD patterns of MBGN, Functionalized MBGN, and *Euphorbia hirta*-loaded MBGN.

Antibacterial activity

The MBGN exhibited marked antibacterial activity, particularly at higher concentrations. MBGN effectively inhibited *Staphylococcus aureus* with a zone of inhibition measuring 28 ± 0.5 mm at 20 µg/mL, and *Acinetobacter baumannii* with an inhibition zone a 14 ± 0.5 mm at 30 µg/mL. In contrast, *Escherichia coli* and *Klebsiella pneumoniae* showed an inhibition zone of 16 ± 0.4 mm at 30 µg/ml and 12 ± 0.5 mm at 20 µg/ml, respectively (Table 1). However, the antibacterial efficacy significantly decreased upon surface functionalization of MBGN. At a concentration of 30µg/ml, functionalized MBGN demonstrated only moderate inhibition against *S. aureus* 18 ± 0.2 mm and weak inhibition against *A.baumannii* 10 ± 0.6 mm. This reduction can be attributed to surface modifications that potentially hindered direct bacterial interaction.

MBGN functionalized with *Euphorbia hirta* extract displayed moderate and concentration-dependent antibacterial activity. Against *S. aureus*, the inhibition zone increased from 11 ± 0.4 mm at 20 µg/ml to 15 ± 0.3 µg/ml, suggesting comparatively low activity. (Table 1) Antibacterial activity of MBGN, Functionalized MBGN, and *Euphorbia hirta*-loaded MBGN against selected bacterial strains. The inhibition zones for both functionalized and *Euphorbia hirta*-loaded MBGN (Figure 7) did not exceed 10 mm against *K.pneumoniae*, confirming limited effectiveness against this Gram-negative strain.

Notably, the *K. pneumoniae* isolated demonstrated the highest resistance, as neither functionalized MBGN nor *Euphorbia hirta*-loaded MBGN exhibited significant antibacterial activity. Similarly, no inhibitory effect was observed against *Pseudomonas aeruginosa* across all MBGN formulations. It is important to note that the agar diffusion assay employed in this study might underestimate antibacterial efficacy, particularly for Gram-negative bacteria, due to its limitations in determining the minimum inhibitory concentration. Future work should incorporate MIC and MBC assays to provide a more quantitative evaluation of antibacterial performance.

Table 1. Comparative Antibacterial activity of MBGN, Functionalized MBGN, *E. hirta-loaded* MBGN against selected pathogens

S.No.	Micro Organisms	Control (Streptomycin 20µg)	Zone of Inhibition (mm)					
			MBGN		Functionalized MBGN		MBGN loaded with *Euphorbia hirta*	
			20µg	30µg	20µg	30µg	20µg	30µg
1	*Staphylococcus aureus*	30	28±0.5	28±0.4	No Zone	18±0.2	11±0.4	15±0.3
2	*Acinetobacter baumannii*	14	No Zone	30±0.5	No Zone	10±0.6	No Zone	11±0.3
3	*Escherichia coli*	26	No Zone	16±0.4	No Zone	10±0.4	No Zone	10±0.2
4	*Klebsiella pneumoniae*	35	No Zone	12±0.5	No Zone	No Zone	No Zone	No Zone
5	*Pseudomonas aeruginosa*	18	No Zone	No Zone	No Zone	No Zone	No Zone	No Zone

(-) – denotes no zone of inhibition observed, indicating that the sample showed no antimicrobial activity.

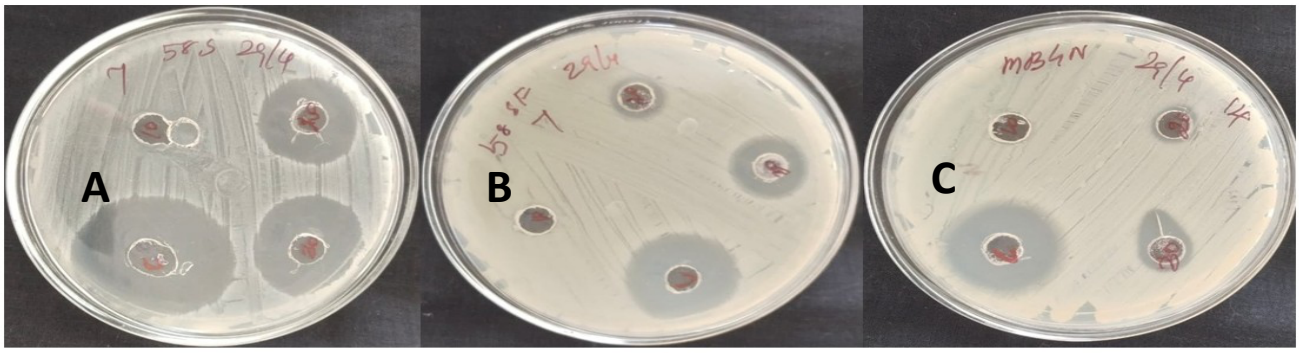

Figure 7. Antibacterial activity of MBGN (A), Functionalized MBGN (B), and *Euphorbia hirta*-loaded MBGN (C) for S. aureus.

Discussion

Euphorbia hirta is a wholesome medicinal herb rich in flavonoids, tannins, terpenoids, quercetin, luteolin, and gallic acid. The repurposing of synthesised metallic nanoparticles using *Euphorbia hirta* has been extensively studied, but its incorporation into mesoporous silica frameworks has not. Additionally, mesoporous bioactive glasses offer a potential delivery vehicle for therapeutic molecules via pore loading or surface functionalization. Hence, in this study, *Euphorbia hirta* was functionalised with MBGNs and characterised to assess their biological properties. The spherical morphology and mesoporous surface architecture of the synthesised MBGNs are consistent with prior reports by Kang et al[18] and Firuzeh et al[17]. Moreover, the study emphasises that pH and hydrolysis rates significantly influenced particle formation during the nucleation and growth phases, which likely explains the observed uniformity and sphericity. *Euphorbia hirta*-loaded MBGNs exhibit markedly increased surface roughness and particle aggregation. These alterations may be attributed to the deposition of organic phytoconstituents from the plant extract onto the nanoparticle surface, forming a heterogeneous bio-coating. The denser surface texture suggested physical adsorption or chemical interactions between the hydroxyl groups of MBGNs and bioactive moieties in *Euphorbia hirta*, potentially enhancing the nanoparticles' biological interface properties.

EDX Analysis revealed the presence of silicon (Si), calcium (Ca), and phosphorus (P), with consistent elemental content before and after functionalization. The strong bands at ~1028–1030 cm^{-1} in all three sample groups are characteristic of asymmetric Si–O–Si stretching vibrations, indicating that the silicate network remains intact. The faint bands at ~790 cm^{-1} and ~693 cm^{-1}, observed exclusively in functionalized and Euphorbia-loaded samples, are attributed to Si–O symmetric stretching and possibly Si–O–C bonding introduced via APTES-mediated functionalization. These spectral shifts validate the successful joining of amino-functional groups and possible interactions with phytochemicals from *Euphorbia hirta*, substantiating similar findings by Nawaz et al [19]

X-ray diffraction patterns further revealed the amorphous nature of all MBGN variants, and the preservation of the amorphous structure following both functionalization and extract loading is essential to maintain the characteristic bioactive dissolution behaviour of MBGNs. This highlights the structural stability of silica-based glasses against surface modifications.

MBGNs alone displayed significant antibacterial activity, particularly against *Staphylococcus aureus* and *Acinetobacter baumannii*, highlighting their intrinsic bioactivity. This could be attributed to the release of Ca^{2+} and silicate ions, which may either disrupt the bacterial membrane or interfere with cell metabolism. Functionalized MBGNs, however, exhibited notably reduced antibacterial efficacy. The poor antibacterial activity of functionalised MBGNs suggests that surface modification via APTES might have hindered effective ion release, resulting in weakened direct contact-based bactericidal action. Thus, the surface functional groups can alter particle–bacteria interactions, potentially forming a barrier against effective biointerface interactions.

Euphorbia hirta-loaded MBGNs demonstrated modest and dose-dependent antibacterial activity, with a maximum zone of inhibition for *S. aureus*. This modest activity could be attributed to the nanoparticle matrix's slow-release kinetics or to insufficient potency at lower concentrations. Specifically, the higher resistance against Gram-negative strains such as *E. coli* and *K. pneumoniae* is due to their outer membrane barriers and efflux mechanisms, as reported in other studies [12]. Notably, none of the formulations showed activity against *Pseudomonas aeruginosa*, emphasising the challenge posed by multidrug-resistant (MDR) organisms and the need for enhanced strategies such as synergistic antibiotic loading or pH-responsive release systems. In human lung adenocarcinoma cells (A549), silver nanoparticles mediated by *Euphorbia hirta* induced apoptosis by modulating the PI3K/Akt/mTOR/p70S6K pathway [21].

Although the ethanolic extract of *Euphorbia hirta* had exhibited antibacterial and antifungal activity against infections, functionalisation with the MBGNs did not show promising activity in our study [22]. Thus, the findings underscore the delicate balance between structural modifications and performance in bioactive glass systems. While functionalization and herbal extract loading can improve biocompatibility or introduce multifunctionality, they may simultaneously compromise core antibacterial properties. To address this challenge, future studies could explore tailoring the APTES chain length or adjusting its density on the MBGNs. This optimization could potentially restore antibacterial potency while preserving loading capacity. These insights can serve as a concrete path for further research, inspiring follow-up studies to enhance ion release and biological activity. Additionally, this study could be further explored for the release kinetics, optimisation of surface chemistry to retain or improve ion release, and the exploration of other biological activities.

Conclusion

This study successfully established the functionalization of MBGNs with *Euphorbia hirta*, which demonstrated that their spherical morphology, mesoporous architecture, and amorphous structure were preserved after surface modification and herbal loading, confirming the structural stability of the glass network. While pristine MBGNs exhibited significant antibacterial activity, particularly against *S.aureus* and *A.baumannii*, surface functionalization with APTES led to a marked reduction in antibacterial efficacy, likely due to hindered ion release and altered particle–bacteria interactions. The *Euphorbia hirta*-loaded MBGNs showed modest, dose-dependent antibacterial activity, indicating that although phytochemical incorporation adds multifunctionality, it may compromise intrinsic bioactivity if not optimally engineered. Overall, the findings underscore the importance of precisely tailoring surface chemistry to balance bioactive ion release and therapeutic loading, and they provide a strong foundation for future optimisation of MBGN-based hybrid nanoplatforms for advanced biomedical applications.

Acknowledgements

Disclosures: The authors have no conflicts of interest.
Acknowledgements: The authors acknowledge the management for research support provided by the Saveetha Institute of Medical and Technical Sciences (SIMATS) Engineering, Saveetha University. The authors sincerely acknowledge Dr K. Sangeetha for providing valuable technical guidance and insightful inputs during the course of this research work.
Funding: None.
Data availability statement: The corresponding author can provide the data supporting the study's conclusions upon request. Due to ethical and privacy constraints, the data are not publicly accessible.

References

1. Li Y, Liu YZ, Long T, Yu XB, Tang TT, Dai KR, et al. Mesoporous bioactive glass as a drug delivery system: fabrication, bactericidal properties and biocompatibility. J Mater Sci: Mater Med. 2013;24(8):1951-61. https://doi.org/10.1007/s10856-013-4960-z
2. Zhao L, Yan X, Zhou X, Zhou L, Wang H, Tang J, et al. Mesoporous bioactive glasses for controlled drug release. Microporous Mesoporous Mater. 2008;109(1-3):210-5. https://doi.org/10.1016/j.micromeso.2007.04.041
3. Awais M, Aizaz A, Nazneen A, Bhatti QuA, Akhtar M, Wadood A, et al. A review on the recent advancements on therapeutic effects of ions in the physiological environments. Prosthesis. 2022;4(2):263-316. https://doi.org/10.3390/prosthesis4020026
4. Hoppe A, Güldal NS, Boccaccini AR. A review of the biological response to ionic dissolution products from bioactive glasses and glass-ceramics. Biomaterials. 2011;32(11):2757-74. https://doi.org/10.1016/j.biomaterials.2011.01.004
5. Wu C, Chang J. Multifunctional mesoporous bioactive glasses for effective delivery of therapeutic ions and drug/growth factors. J Controlled Release. 2014;193:282-95. https://doi.org/10.1016/j.jconrel.2014.04.026
6. Bae EJ, Park HJ, Park JS, Yoon JY, Kim YH, Choi KH, et al. Effect of chemical stabilizers in silver nanoparticle suspensions on nanotoxicity. Bull Korean Chem Soc. 2011;32(2):613-9. https://doi.org/10.5012/bkcs.2011.32.2.613
7. Baram-Pinto D, Shukla S, Perkas N, Gedanken A, Sarid R. Inhibition of herpes simplex virus type 1 infection by silver nanoparticles capped with mercaptoethane sulfonate. Bioconjugate Chem. 2009;20(8):1497-502. https://doi.org/10.1021/bc900215b

8. Galdiero S, Falanga A, Vitiello M, Cantisani M, Marra V, Galdiero M. Silver nanoparticles as potential antiviral agents. Molecules. 2011;16(10):8894-918. https://doi.org/10.3390/molecules16108894
9. Sun L, Singh AK, Vig K, Pillai SR, Singh SR. Silver nanoparticles inhibit replication of respiratory syncytial virus. J Biomed Nanotechnol. 2008;4(2):149-58. https://doi.org/10.1166/jbn.2008.012
10. Xiang Dx, Chen Q, Pang L, Zheng Cl. Inhibitory effects of silver nanoparticles on H1N1 influenza A virus in vitro. J Virol Methods. 2011;178(1-2):137-42. https://doi.org/10.1016/j.jviromet.2011.09.003
11. Khursheed A, Jain V. Euphorbia hirta as a gold mine of high-value phytochemicals: A comprehensive review of its pharmacological activities and possible role against SARS-CoV-2. Biomed Res Ther. 2022;9(2):4930-49. https://doi.org/10.15419/bmrat.v9i2.728
12. Ilyas K, Singer L, Akhtar MA, Bourauel CP, Boccaccini AR. Boswellia sacra extract-loaded mesoporous bioactive glass nanoparticles: synthesis and biological effects. Pharmaceutics. 2022;14(1):126. https://doi.org/10.3390/pharmaceutics14010126
13. Asha S, Thirunavukkarasu P, Mohamad Sadiq A. Phytochemical screening of Euphorbia hirta linn leaf extracts. World J Pharm Sci. 2015;:1104-12.
14. Ogbulie J, Ogueke C, Okoli IC, Anyanwu BN. Antibacterial activities and toxicological potentials of crude ethanolic extracts of Euphorbia hirta. Afr J Biotechnol. 2007;6(13).
15. Zarghami V, Ghorbani M, Bagheri KP, Shokrgozar MA. Prolongation of bactericidal efficiency of chitosan—Bioactive glass coating by drug controlled release. Prog Org Coat. 2020;139:105440. https://doi.org/10.1016/j.porgcoat.2019.105440
16. Bibi M, Batool SA, Iqbal S, Zaidi SB, Hussain R, Akhtar M, et al. Synthesis and characterization of mesoporous bioactive glass nanoparticles loaded with peganum harmala for bone tissue engineering. Heliyon. 2023;9(11). https://doi.org/10.1016/j.heliyon.2023.e21636
17. Firuzeh M, Labbaf S, Sabouri Z. A facile synthesis of mono-dispersed, spherical and mesoporous bioactive glass nanoparticles for biomedical applications. J Non-Cryst Solids. 2021;554:120598. https://doi.org/10.1016/j.jnoncrysol.2020.120598
18. Kang MS, Lee NH, Singh RK, Mandakhbayar N, Perez RA, Lee JH, et al. Nanocements produced from mesoporous bioactive glass nanoparticles. Biomaterials. 2018;162:183-99. https://doi.org/10.1016/j.biomaterials.2018.02.005
19. Nawaz Q, Rehman MAU, Burkovski A, Schmidt J, Beltrán AM, Shahid A, et al. Synthesis and characterization of manganese containing mesoporous bioactive glass nanoparticles for biomedical applications. J Mater Sci: Mater Med. 2018;29(5):64. https://doi.org/10.1007/s10856-018-6070-4
20. Tabia Z, El Mabrouk K, Bricha M, Nouneh K. Mesoporous bioactive glass nanoparticles doped with magnesium: drug delivery and acellular in vitro bioactivity. RSC Adv. 2019;9(22):12232-46. https://doi.org/10.1039/C9RA01133A
21. Jiménez-González V, Kowalczyk T, Piekarski J, Szemraj J, Rijo P, Sitarek P. Nature's green

potential: anticancer properties of plants of the Euphorbiaceae family. Cancers. 2023;16(1):114. https://doi.org/10.3390/cancers16010114

22. Parmar G, Pundarikakshudu K, Balaraman R, Sailor G. Amelioration of anaphylaxis, mast cell degranulation and bronchospasm by Euphorbia hirta L. extracts in experimental animals. Beni-Suef Univ J Basic Appl Sci. 2018;7(1):127-34. https://doi.org/10.1016/j.bjbas.2017.11.001